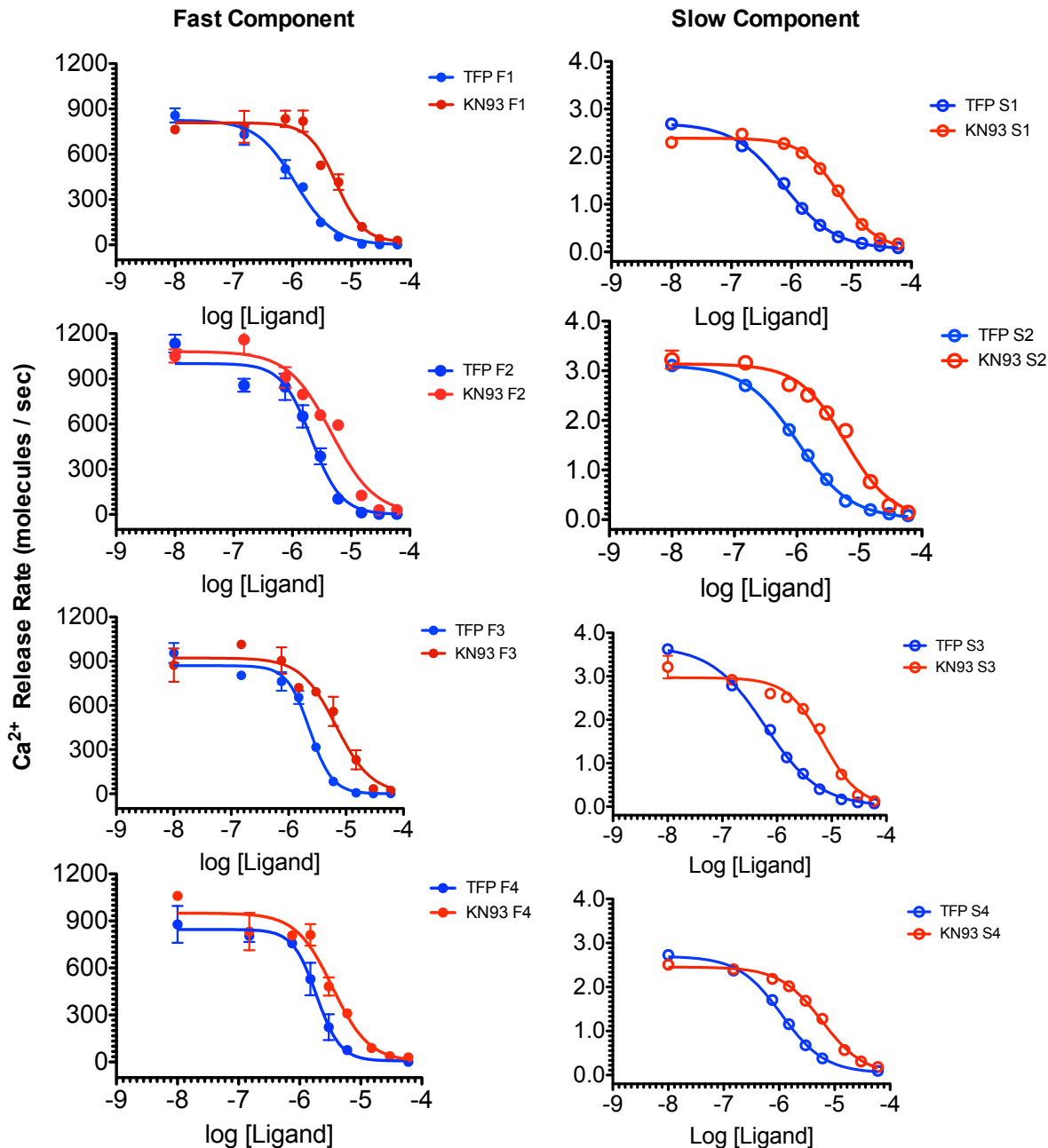


**Table S1. CaM Ca<sup>2+</sup> release rates determined by Quin-2 fluorescence using stopped-flow during TFP and KN93 titrations.** During each titration, each data point was collected a minimum of two times and the values were averaged. EC<sub>50</sub> and Hill slope are reported in the text as the mean average ± standard deviation. Error bars on the plots below are shown as standard error of measurement for each titration data point.

| Exp # | Fast EC <sub>50</sub> |          | Slow EC <sub>50</sub> |          | Fast Hill Slope |       | Slow Hill Slope |       |
|-------|-----------------------|----------|-----------------------|----------|-----------------|-------|-----------------|-------|
|       | TFP                   | KN93     | TFP                   | KN93     | TFP             | KN93  | TFP             | KN93  |
| R1    | 1.10E-06              | 5.46E-06 | 7.55E-07              | 6.25E-06 | -1.32           | -1.86 | -1.02           | -1.39 |
| R2    | 2.12E-06              | 4.64E-06 | 1.03E-06              | 6.00E-06 | -1.71           | -1.17 | -1.03           | -1.16 |
| R3    | 2.33E-06              | 6.71E-06 | 6.12E-07              | 6.92E-06 | -2.20           | -1.41 | -0.88           | -1.31 |
| R4    | 1.89E-06              | 3.45E-06 | 1.11E-06              | 5.90E-06 | -2.22           | -1.45 | -1.12           | -1.14 |



**Table S2. Data collection and refinement statistics.**

|                                       | CaM-KN93                        |
|---------------------------------------|---------------------------------|
| <b>Wavelength</b>                     | 0.978                           |
| <b>Resolution range</b>               | 35.08 - 1.6 (1.657 - 1.6)       |
| <b>Space group</b>                    | P 61 2 2                        |
| <b>Unit cell</b>                      | 40.511 40.511 348.785 90 90 120 |
| <b>Total reflections</b>              | 48058 (4506)                    |
| <b>Unique reflections</b>             | 24029 (2252)                    |
| <b>Multiplicity</b>                   | 2.0 (2.0)                       |
| <b>Completeness (%)</b>               | 99.79 (98.95)                   |
| <b>Mean I/sigma(I)</b>                | 14.63 (2.21)                    |
| <b>Wilson B-factor</b>                | 19.96                           |
| <b>R-merge</b>                        | 0.03894 (0.2091)                |
| <b>R-meas</b>                         | 0.05507 (0.2957)                |
| <b>R-pim</b>                          | 0.03894 (0.2091)                |
| <b>CC1/2</b>                          | 0.996 (0.884)                   |
| <b>CC*</b>                            | 0.999 (0.969)                   |
| <b>Reflections used in refinement</b> | 24007 (2252)                    |
| <b>Reflections used for R-free</b>    | 1799 (169)                      |
| <b>R-work</b>                         | 0.2315 (0.3115)                 |
| <b>R-free</b>                         | 0.2742 (0.3444)                 |
| <b>CC(work)</b>                       | 0.945 (0.733)                   |
| <b>CC(free)</b>                       | 0.909 (0.620)                   |
| <b>Number of non-hydrogen atoms</b>   | 1391                            |
| <b>macromolecules</b>                 | 1164                            |
| <b>ligands</b>                        | 106                             |
| <b>solvent</b>                        | 121                             |
| <b>Protein residues</b>               | 147                             |
| <b>RMS(bonds)</b>                     | 0.005                           |
| <b>RMS(angles)</b>                    | 0.90                            |
| <b>Ramachandran favored (%)</b>       | 97.93                           |
| <b>Ramachandran allowed (%)</b>       | 2.07                            |
| <b>Ramachandran outliers (%)</b>      | 0.00                            |
| <b>Rotamer outliers (%)</b>           | 1.59                            |
| <b>Clashscore</b>                     | 5.51                            |
| <b>Average B-factor</b>               | 34.34                           |
| <b>macromolecules</b>                 | 32.20                           |
| <b>ligands</b>                        | 54.77                           |
| <b>solvent</b>                        | 37.08                           |

Statistics for the highest-resolution shell are shown in parentheses.

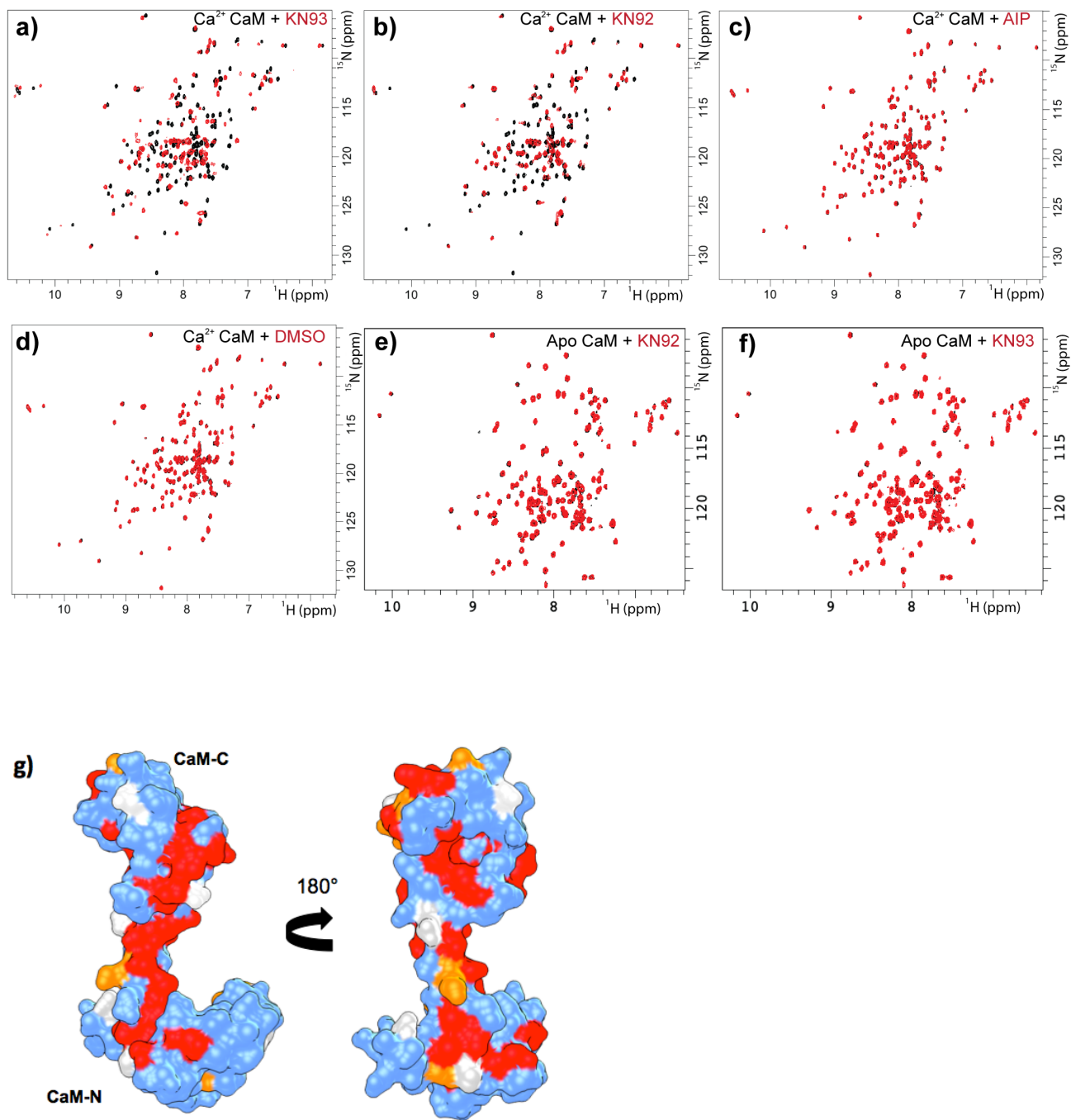


**Figure S1. Biophysical characterization of CaM-KN interactions by NMR.** Overlay of 2D  $^{15}\text{N}$   $^1\text{H}$  HSQC NMR spectra of CaM in the absence (black) and presence (red) of: **(a)** 1 : 4 molar ratio CaM : KN93, **(b)** 1 : 4 molar ratio CaM : KN92, **(c)** 1 : 4 molar ratio CaM : AIP and **(d)** 20  $\mu\text{l}$  of DMSO in the presence of  $\text{Ca}^{2+}$ . Overlay of 2D  $^{15}\text{N}$   $^1\text{H}$  HSQC NMR spectra of apo CaM in the absence (black) and presence of **(e)** 1 : 2 molar ratio CaM : KN92 **(f)** 1 : 2 molar ratio CaM : KN93. Significant differences are not observed for any of CaM's resonance frequencies in panels c-f. **(g)** Surface rendering of CaM (PDB ID: 1CLL) color coded by extent of chemical shift perturbation upon the addition of KN93 (**unaffected**, **moderate**, **strong**). Resonances that could not be distinguished due to overlap in the presence of KN93 are shown in white. **(h)** Plot of chemical shift perturbation vs. CaM residues.

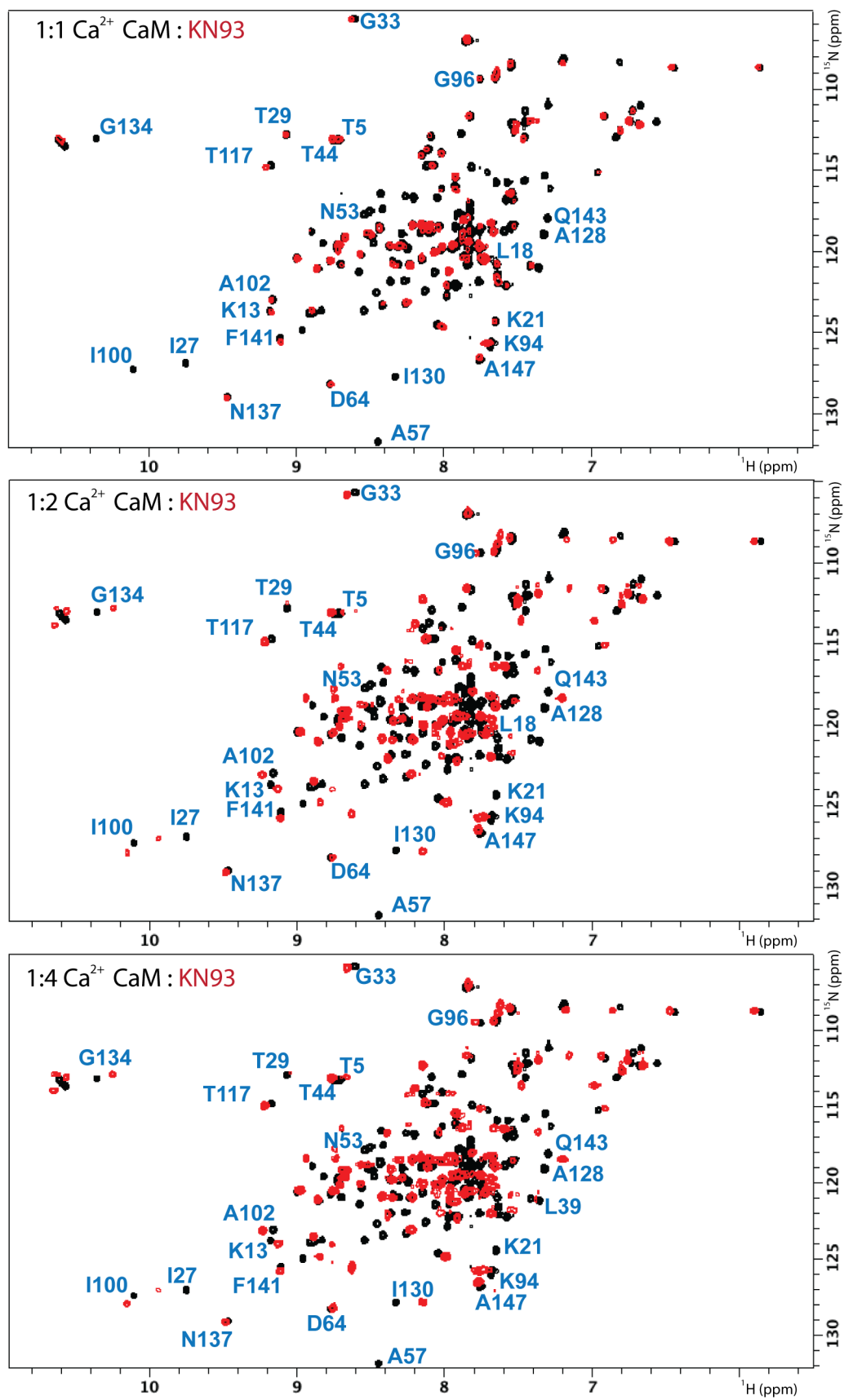


**Figure S2.** Overlay of 2D <sup>1</sup>H-<sup>15</sup>N HSQC NMR spectra collected during a titration of isotopically enriched <sup>15</sup>N CaM (black) with KN93 (red).

Electron density map (2Fo-Fc)

Omit map (Fo-Fc)

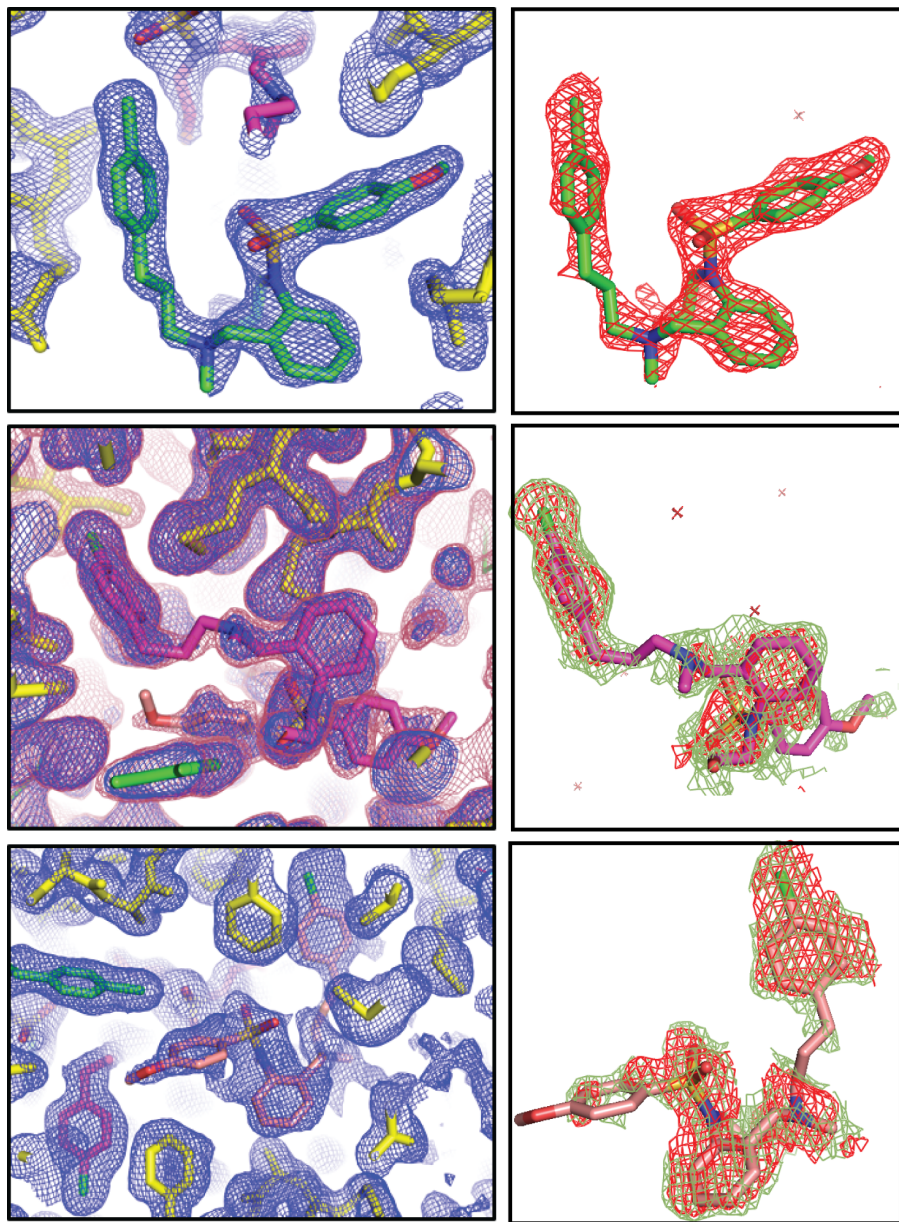


**Figure S3 . CaM-KN93 complex; electron density for the three molecules of KN93.** (Left) 2Fo – Fc map of electron density at 1 sigma. (Right) Fo-Fc omit map in the absence of KN93 molecules (calculated using omit map protocol, phenix program package). Omit densities are shown at 2 sigma (red) and 1.2 sigma (light green). KN93 molecules are displayed as follows: 201 (green) 202 ,(purple) and 203 (pink).

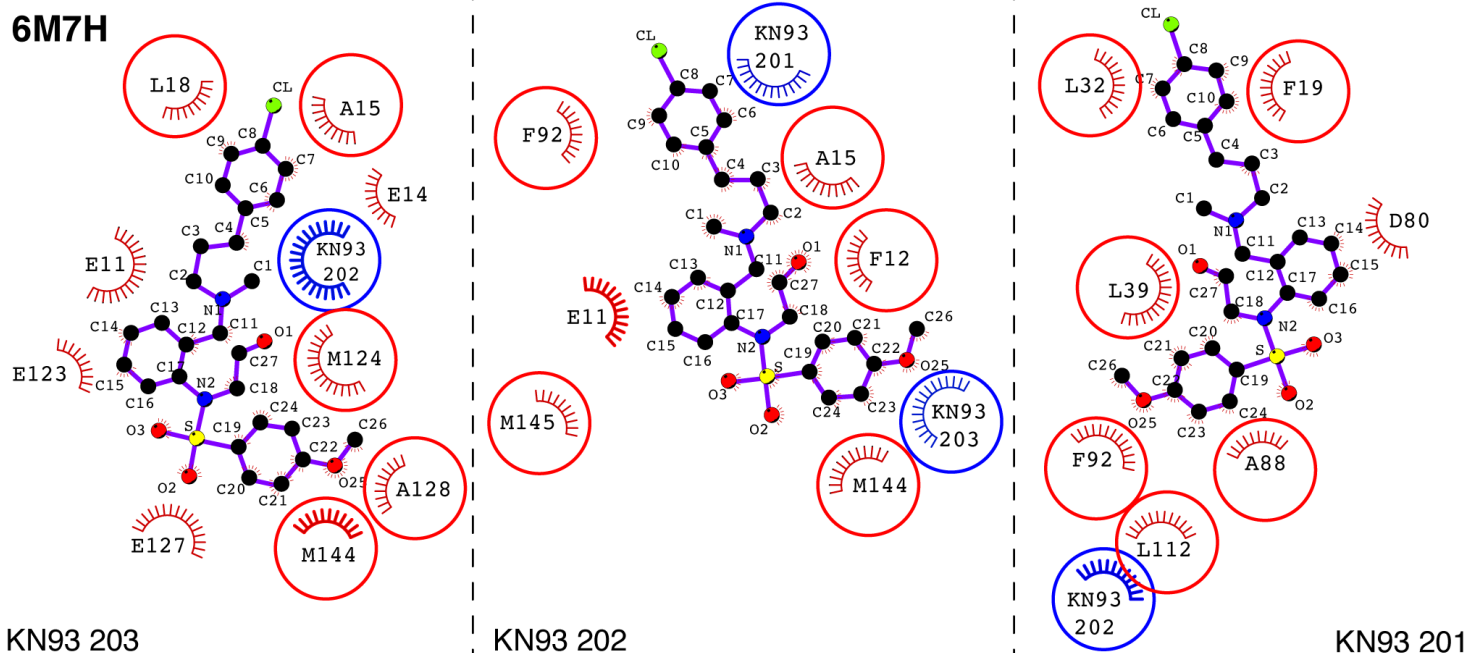


**Figure S4. LigPlot of CaM-KN93 complex (PDB ID 6M7H) showing all side chain contacts within 4 Å of each KN93 binding interface.** Hydrophobic CaM side chains are circled in red and contacts with other KN93 molecules are in circled blue. For CaM-TFP interactions the rotamer conformation of CaM M144 has been suggested to play a part in determining the binding orientation of TFP [1]. Our crystal structure of CaM-KN93 also contains a similar CaM contact suggesting the conformation of the M144 side chain may also influence the binding orientation of KN93.

- [1] M.D. Feldkamp, L. Gakhar, N. Pandey, M.A. Shea, Opposing orientations of the anti-psychotic drug trifluoperazine selected by alternate conformations of M144 in calmodulin, *Proteins Struct. Funct. Bioinforma.* 83 (2015) 989–996. doi:10.1002/prot.24781.



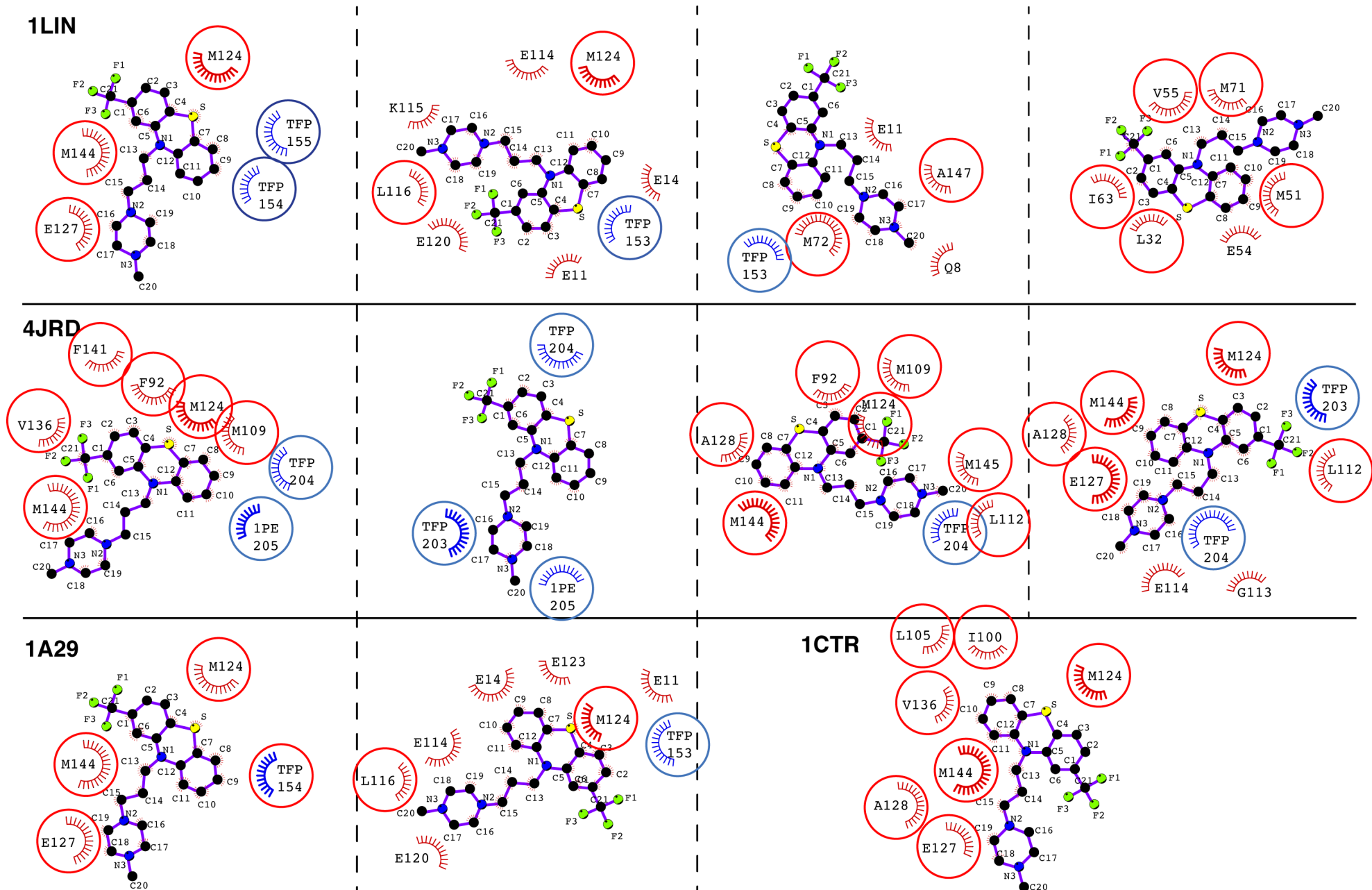


**Figure S5. LigPlot analysis for the four available crystal structures of CaM-TFP.** Hydrophobic CaM side chains and other TFP molecules within 4 Å of each TFP binding interface are labeled and circled in red and blue respectively. Several TFP binding orientations and stoichiometries are observed in the different the crystal structures. Similarly it is likely CaM can accommodate KN93 binding in multiple conformations and different stoichiometries depending on the solution conditions.

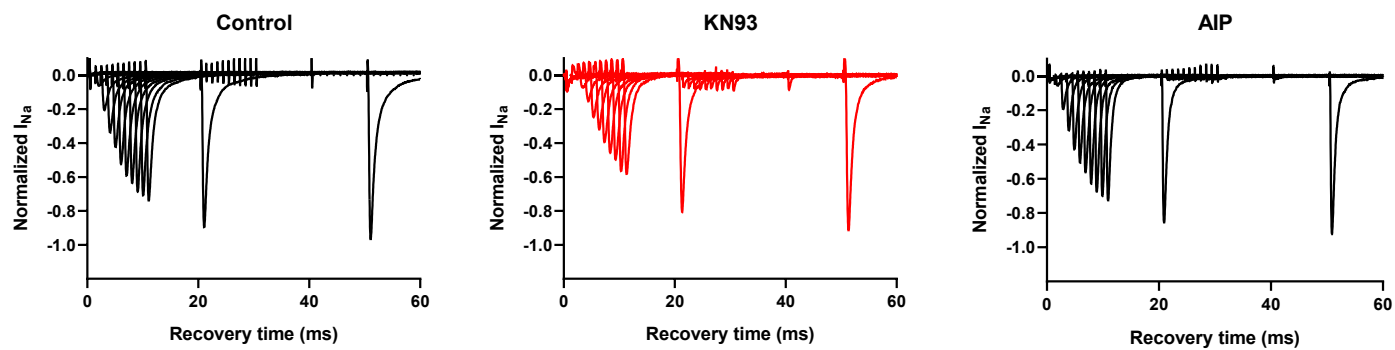


**Figure S6. Representative traces for recovery from inactivation in the presence of DMSO (control), KN93, or AIP.** Pulse protocols are shown in figure 3 panel A.



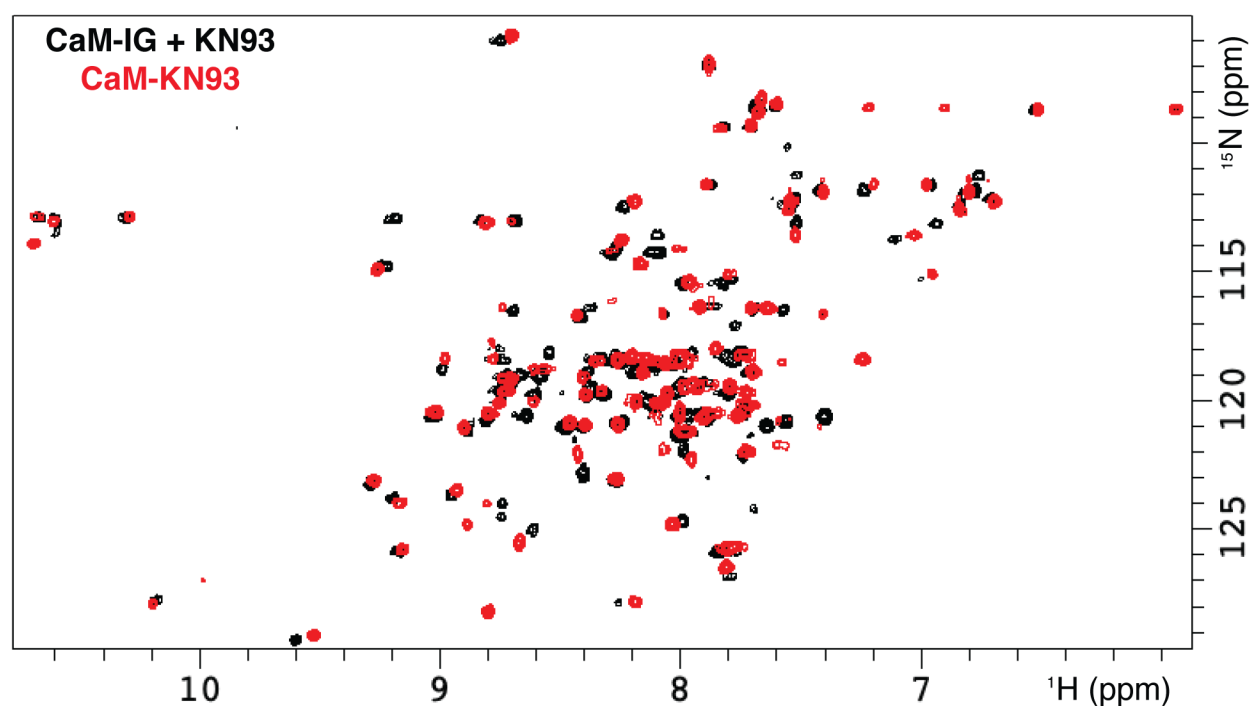
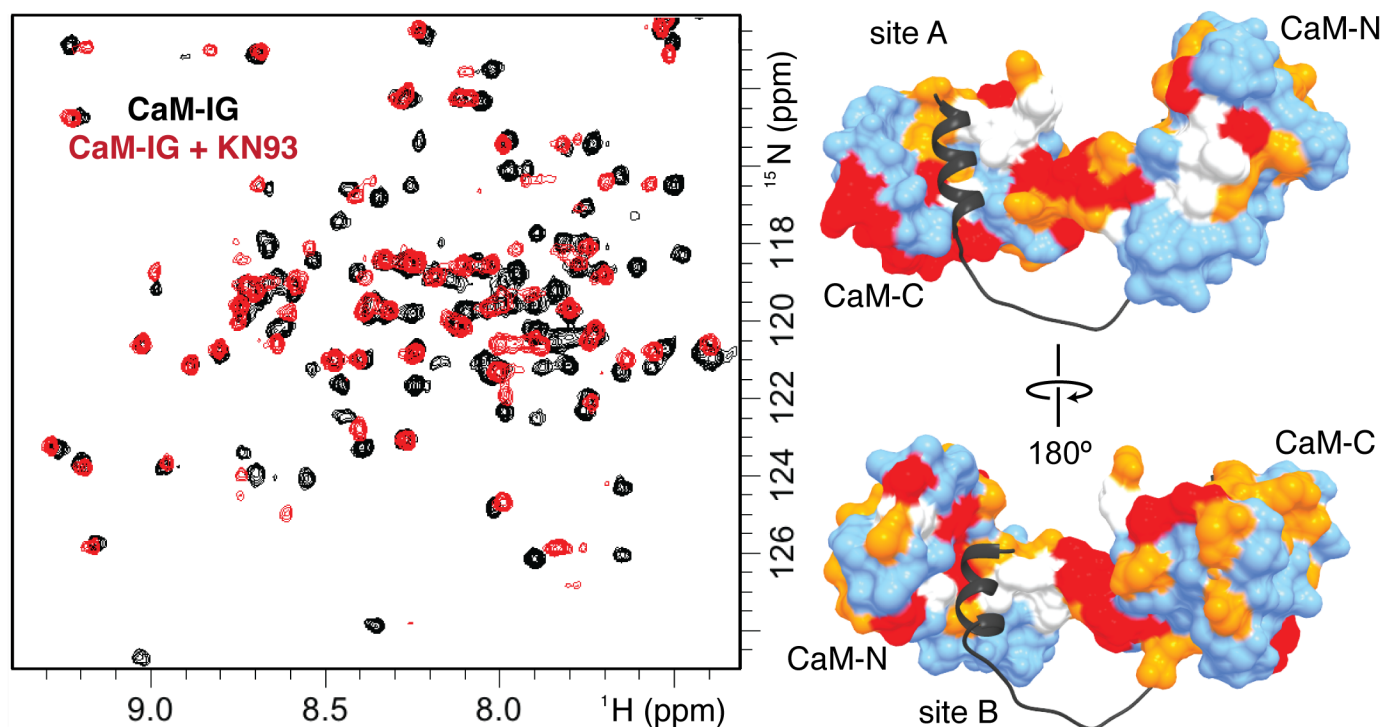


**Figure S7. KN93 modifies CaM's interaction with the Nav1.5 IG.** Overlay of  $^{15}\text{N}$ - $^1\text{H}$  HSQC NMR spectra of isotopically enriched  $^{15}\text{N}$  CaM bound to IG peptide in the absence (black) and presence of KN93 (red) (top left). Structural model of the CaM-IG complex [16] with surface rendering of CaM color coded by extent of chemical shift perturbation (**strong**, **moderate**, **unaffected**) upon the addition of KN93 (top right). Chemical shifts that could not be clearly distinguished due to overlap are shown in white (top right). Overlay of 2D  $^{15}\text{N}$ - $^1\text{H}$  HSQC **CaM-IG-KN93** (black) with **CaM-KN93** spectra (red) reveals that KN93 does not replace the Nav1.5 inactivation gate but instead forms a ternary complex (bottom). NMR spectra, CSP plots, and TALOS calculations for  $\text{Ca}^{2+}$  CaM in the absence and presence of the IG construct are reported in Johnson et al. Structure 2018.

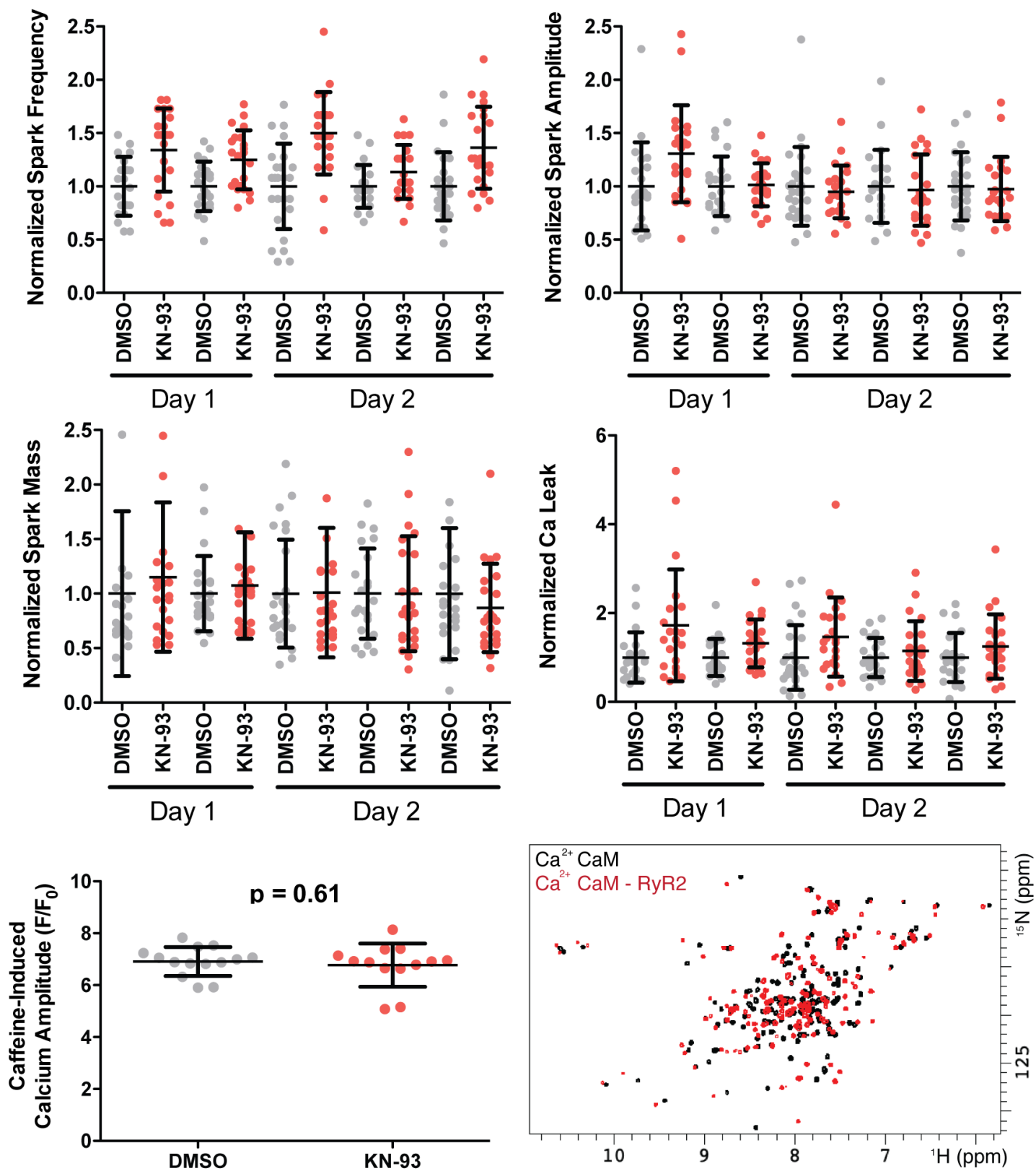


**Figure S8. Summary of all RyR2 spark mediate  $\text{Ca}^{2+}$  release data.** In all experiments the addition of KN93 consistently increased spark frequency without significant effects to the spark mass or amplitude (top). SR content between the groups was not significantly altered by the addition of KN93 (lower left). Overlay of 2D HSQC NMR spectra of isotopically enriched  $^{15}\text{N}$  CaM in the absence (black) and presence (red) of RyR2 peptide (lower right) displays numerous chemical shift perturbations, consistent with both domains of CaM interacting with the RyR2 peptide in the presence of  $\text{Ca}^{2+}$ .